ACS Catalysis

Letter

pubs.acs.org/acscatalysis

Tracing Active Sites in Supported Ni Catalysts during Butene Oligomerization by *Operando* Spectroscopy under Pressure

Jabor Rabeah,*[,†] Jörg Radnik,[†] Valérie Briois,[‡] Dietrich Maschmeyer,[§] Guido Stochniol,[§] Stephan Peitz,[§] Helene Reeker,[§] Camille La Fontaine,[‡] and Angelika Brückner*[,†]

[†]Leibniz-Institut für Katalyse e. V., an der Universität Rostock, Albert-Einstein-Straße 29a, D-18059 Rostock, Germany

[‡]SOLEIL Synchrotron, UR1-CNRS, L'Orme des Merisiers, BP48, Saint-Aubin 91192, Gif-sur Yvette, France

[§]Evonik Performance Materials GmbH, Paul-Baumann-Str. 1, 45772 Marl, Germany

Supporting Information

ABSTRACT: Supported Ni catalysts have been studied during the dimerization of butenes by *operando* electron paramagnetic resonance (EPR) and *in situ* X-ray absorption spectroscopy (XAS) at 353 K and up to 16 bar. Single Ni^{I}/Ni^{II} shuttles were identified as active sites, whereby the conversion of initial Ni^{I} to Ni^{II} by oxidative addition of butene is obviously faster than the re-reduction of Ni^{II} to Ni^{I} by reductive elimination of the C8 product, rendering the equilibrium percentage of Ni^{I} small. At $p \leq 2$ bar, Ni^{I} single sites form inactive Ni^{0} aggregates, while this is suppressed at higher pressure (~12 bar). A reaction mechanism is proposed.

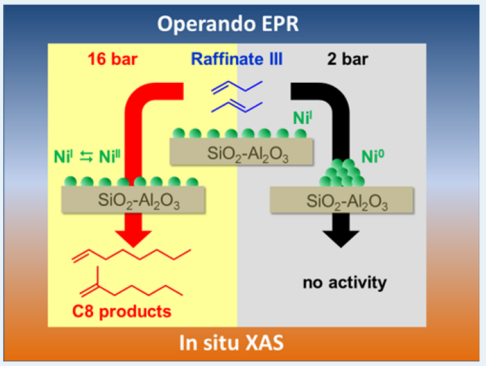

KEYWORDS: *operando EPR, in situ EXAFS/XANES, heterogeneous catalysis, butene dimerization, reaction mechanism, nickel catalysts*

The dimerization of *n*-butenes is the industrial basis for higher olefins being important building blocks for plasticizer production.[1] The heterogeneous OCTOL process uses a NiO catalyst supported on Al_2O_3–SiO_2 (SiAl) and the C4 fraction from the steam cracker (raffinate III) as feedstock at 25–35 bar.[2,3] However, some years ago, we found that Ni/SiAl catalysts with Ni loadings of <1% show similar performance as the commercial NiO/SiAl catalyst.[2] This result, together with the fact that the product distribution is very similar to that in the homogeneous DIMERSOL process,[2] suggested that active sites in Ni/SiAl catalysts may be single Ni^{I} sites, probably single Ni^{I}–H species formed via the reaction of the Ni precursor with Brønsted sites of the SiAl support.

Indeed, we could show previously, by electron paramagnetic resonance (EPR) that such sites can be formed in <1% Ni/SiAl catalysts and that their agglomeration to Ni^{0} clusters causes deactivation.[2] However, it was not possible at that time to derive a reliable relationship between the amount of such Ni^{I} single sites and the catalytic performance since, despite utmost caution, the reproducibility of the preparation method was too low and damage of the extremely air- and moisture-sensitive Ni^{I} single sites, upon transfer of the catalyst between the glovebox, reactor, and EPR sample tube could not be completely excluded. Apart from this drawback, another important question still remained open, namely, whether EPR-silent species such as Ni^{II} and/or Ni^{I}–Ni^{I} dimers are possibly formed during reaction and could work as active sites.

In this work, we achieved a breakthrough in identifying structure–reactivity relationships in Ni-catalyzed butene dimerization by developing a reproducible method to stabilize Ni^{I} single sites on supports of different acidity, based on the synproportionation of bis(cyclopentadienyl)nickel(II) [$Ni^{II}(Cp)_2$] with bis(1,5-cyclooctadiene)nickel(0) [$Ni^{0}(COD)_2$]. Moreover, we have established an advanced *operando* EPR setup by which the possible (detrimental) formation of Ni^{0} clusters can be monitored under reaction conditions (~350 K and up to 20 bar), while single Ni^{I} sites (detectable only at low temperature) are analyzed without removing the catalyst from the reactor after temporal quenching to ~100 K in different states of activity and selectivity (Figure S1 in the Supporting Information). To check for EPR-silent species such as single Ni^{II} and/or Ni^{I}–Ni^{I} dimers, *in situ* X-ray absorption near-edge structure (XANES) and extended X-ray absorption fine structure (EXAFS) measurements were performed under the same conditions of temperature and pressure (Figure S2 in the Supporting Information). To the best of our knowledge, these studies are currently the only examples of *operando* EPR combined with *in situ* X-ray absorption spectroscopy (XAS) under elevated pressure in catalytic liquid/solid systems.

Received: August 15, 2016
Revised: September 26, 2016
Published: November 4, 2016

DOI: 10.1021/acscatal.6b02331
ACS Catal. 2016, 6, 8224–8228

To ensure reliable assignment of reaction-dependent changes of the Ni^I EPR signal, the 0.6% Ni/SiAl catalyst was first exposed to increasing pressure of 1-butene at 293 K, followed by recording the EPR spectra at 77 K (Figure 1). The

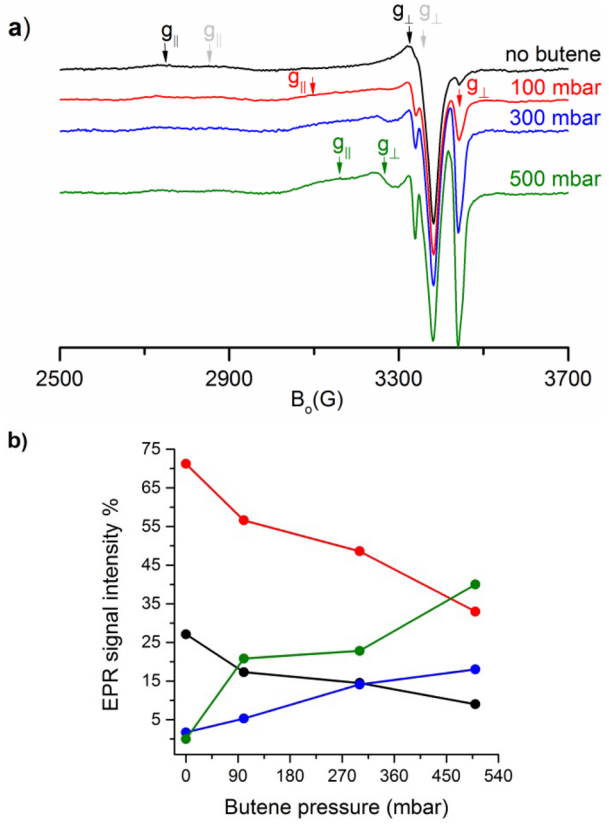

Figure 1. (a) EPR spectra of 0.6% Ni/SiAl after exposure to different pressures of 1-butene. Arrows denote *g*-tensor components of the different Ni^I subsignals S1−S4 derived by spectra simulation (see Figure S3 and Table S1): for S1 (black): $g_{\parallel}$ = 2.536, $g_{\perp}$ = 2.069; for S2 (gray): $g_{\parallel}$ = 2.443, $g_{\perp}$ = 2.051; for S3 (red): $g_{\parallel}$ = 2.219, $g_{\perp}$ = 2.012; and for S4 (green): $g_{\parallel}$ = 2.233, $g_{\perp}$ = 2.090. (b) Relative intensity of components S1 (black), S2 (red), S3 (blue), and S4 (green) with regard to dependence on the pressure of 1-butene (Table S1).

corresponding simulated spectra, together with the derived g-tensor parameters, are shown in the Supporting Information (Figure S3 and Table S1). Without butene, two axial signals of single Ni^I sites are observed, which differ slightly in their spin Hamiltonian parameters (signal 1: $g_{\parallel}$ = 2.536, $g_{\perp}$ = 2.069; signal 2: $g_{\parallel}$ = 2.443, $g_{\perp}$ = 2.051, derived by spectra simulation; see Figure S3 in the Supporting Information). We assign these lines to Ni^I species at different positions of the support (possibly near Si or Al), which may still contain Cp and/or chemical oxygen demand (COD) ligands. Remarkably, no signal of ferromagnetic Ni^0 is seen, indicating that the new preparation route effectively suppresses agglomeration of single Ni^I sites (which was almost always observed in previous investigations[2]).

Under 1-butene, two additional signals appear: site 3 ($g_{\parallel}$ = 2.219, $g_{\perp}$ = 2.012) is attributed to Ni^I, which coordinates to a π-system, since a similar shift to lower *g*-values has been found for Ni^I interacting with π-electrons of unsaturated hydrocarbons.[4,5] It may arise from a Ni site that forms a π-complex with 1-butene. The $g_{\perp}$ value of signal 4 ($g_{\parallel}$ = 2.233, $g_{\perp}$ = 2.090) is much larger, in comparison to those of signals 1−3, suggesting that signal 4 does not arise from a π-complex of Ni^I with 1-butene but rather from a Ni^I−$(CH_2)_3CH_3$ complex formed by insertion of 1-butene into the Ni−H bond, which is commonly assumed to be the first step in the reaction cycle.[6−8] Signals 1 and 2 decrease with rising butene pressure, in favor of signals 3 and 4 (see Figure 1b, as well as Table S1), indicating that those Ni^I species (Ni^I···Cp and/or Ni^I···COD) are converted to species 3 (Ni^I···π) and 4 (Ni^I−$(CH_2)_3CH_3$).

During reaction with raffinate III (composition: 0.1% isobutane, 25.3% *n*-butane, 26.6% *trans*-butene, 14.7% *cis*-butene, and 33% 1-butene), 1-butene is mainly isomerized to *trans*-butene (Figure 2a). This process is preferentially

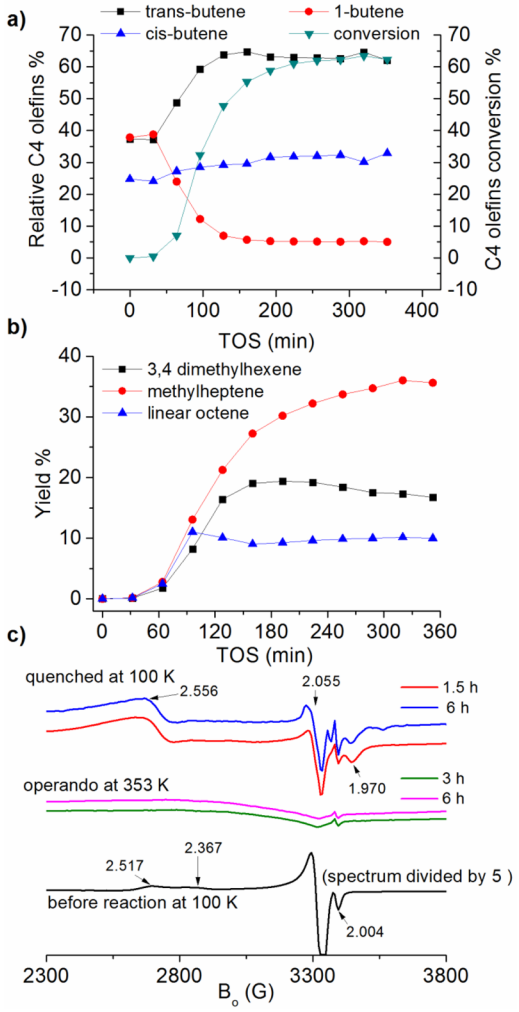

Figure 2. (a) C4 conversion and relative percentage of C4 olefins; (b) C8 yield; and (c) EPR spectra under reaction conditions (pink and green, 353 K, 16 bar) and after quenching the reaction to 100 K and 5 bar at 1.5 h and at 6 h (red and blue), in comparison to the as-prepared catalyst (black).

catalyzed by acidic sites.[9,10] It also occurs, to a certain extent, on Ni-free acidic supports,[11] while Ni^I species on a nonacidic support (SiO_2) showed neither isomerization nor dimerization activity. The C4 conversion increases and C8 products are formed with time (Figure 2b) via a Ni-catalyzed mechanism.[3,12] Figure 2c shows EPR spectra after 1.5 h, when isomerization was still significant (Figure 2a) and after 6 h under proper oligomerization conditions. The *operando* EPR spectra recorded at 353 K and 16 bar (Figure 2c) show only a very weak and broad signal of ferromagnetic Ni^0 at *g* = 2.20, which

DOI: 10.1021/acscatal.6b02331
ACS Catal. 2016, 6, 8224−8228

did not change with the time on stream (TOS), while the catalyst remained active. Since Ni^{I} can only be seen at low temperature, because of the short relaxation time, the reactor had to be quenched to 100 K.

In comparison to the as-prepared catalyst, a significant decrease in the total Ni^{I} intensity was already observed after 1.5 h TOS and the shape of the Ni^{I} signal did not change for up to 6 h TOS, indicating that the Ni^{I} species present after 1.5 h remains unchanged during further reaction up to 6 h TOS. The $g_{\|}$ components of the initial Ni^{I} signals merge in a broad feature at $g_{\|} = 2.556$, while the perpendicular components at $g_{\perp} = 2.055$ and 2.004 remain almost constant. This points to a higher axial distortion of the Ni^{I} symmetry under reaction conditions, which might arise from a change in the coordination environment, probably due to replacement of the Cp and/or COD ligands by C4.

Interestingly, a new signal appeared at $g_{\perp} = 1.970$, which is unusually low for Ni^{I}. According to theory, all g-tensor components of a Ni^{I} ion ($S = {}^{1}/_{2}$, d^{9}) should be larger than the free-electron g-value ($g = 2.0023$).[13] A shift to lower field has been attributed to the interaction of the Ni d-electrons with the π-electrons of olefin ligands.[14−16] Thus, Ni^{I} signals with components at 1.985 and 1.971 have been assigned to Ni^{I}-ethylene complexes formed after ethylene adsorption in Ni-containing clinoptinolite[15] and a signal at $g = 1.965$ was observed after adsorption of ethylene on a Ni−Y zeolite.[16] After the adsorption of *trans*-2-butene on a $NiO/Al_2O_3-SiO_2$ catalyst, even-lower g-values of 1.938, 1.880, and 1.879 have been observed for the formed Ni^{I} species.[14] In a [(bpy)Ni-(mesityl)$_2$] complex, such a low $g_{\perp}$ value was explained by a partial shift of electron density from Ni into the π^* orbitals of the ligands.[17] The $g_{\perp} = 1.970$ signal in Figure 2c probably arises from the adsorption of more than one butene molecule on the same Ni^{I} site.

The Ni^{I} EPR intensity already decreases by ∼85% after 1.5 h TOS. This suggests the conversion of Ni^{I} to EPR-silent species. To identify such EPR-silent sites, *in situ* XANES/EXAFS measurements (at 353 K and 12.4 bar) have been performed. The absorption edge energy in the XANES spectrum of the 0.6% Ni/SiAl catalyst before exposure to raffinate ($E_{0.35}$) is between that of the references Ni^{0} foil and NiO, suggesting that monovalent Ni^{I} is the dominating Ni species (see Figure 3).

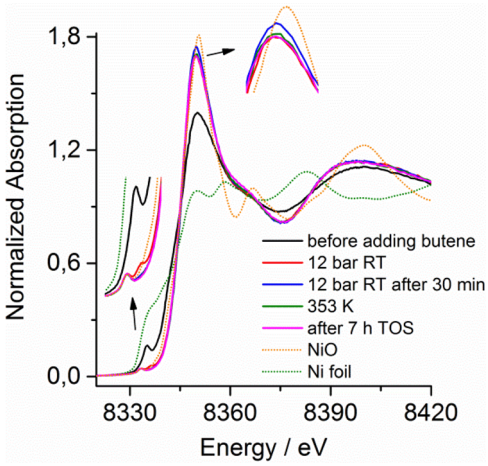

Figure 3. Normalized *in situ* XANES spectra of 0.6% Ni/SiAl in as-prepared form, after exposure to raffinate III at 12.4 bar and room temperature and subsequent heating to 353 K.

This is in good agreement with EPR results. When the catalyst is exposed to raffinate III at 12.4 bar and room temperature (RT), the absorption edge is shifted to higher energy and the intensity of the white line increases, suggesting oxidation of Ni^{I} to Ni^{II}, which continues with time (red and blue lines in Figure 3). However, the Ni edge is still somewhat far from that of the NiO reference, suggesting that not all Ni^{I} species are oxidized to Ni^{II}. In addition, the pre-edge peak at 8335 eV shifted to higher energy (8336 eV), decreased in intensity, and finally vanished after 30 min at RT while a new weak peak appeared at 8333.7 eV. This is assigned to the 1s → 3d transition, which is forbidden by the selection rule but can gain some intensity due to the 3d+4p mixing in non-centrosymmetric Ni compounds.[18,19] This indicates that the Ni coordination changes already at RT, probably because of the removal of COD/CP ligands and adsorption of butenes. However, it is not possible to deduce the precise geometry of the Ni sites just from the pre-edge features, since different coordination numbers (CNs) can give rise to similar peaks, although with different transition probabilities.[20,21] Thus, it has been observed that the coordination of one or two additional ligands to square-planar Ni^{I} and Ni^{II} complexes just leads to an attenuation of the pre-edge peak at 8335 eV, resulting from the 1s → 4p transition.[22] The pre-edge peak at 8336 disappeared after 30 min at RT, while that at 8333.7 eV remained almost unchanged during TOS, probably due to complete exchange of COD/CP ligands at the Ni sites by butenes to form an ∼6-fold-coordinated Ni species. This is also suggested by the EXAFS data discussed below. Upon heating to the reaction temperature of 353 K, the white line dropped slightly, indicating that only a small part of Ni^{II} is reduced again. This is consistent with the EPR results, where a decrease in the EPR intensity of the Ni^{I} signal was always observed after reaction (see Figure 2c).

From EXAFS, the distances between Ni and the neighboring atoms, as well as the coordination number and the type of the surrounding atoms can be determined. Ni−O−Ni and/or Ni−Ni interactions typical for NiO or Ni clusters were not observed, which confirms the presence of Ni single sites (see Figure 4). Because of the quality of the EXAFS data, fits are limited to the first shell only.

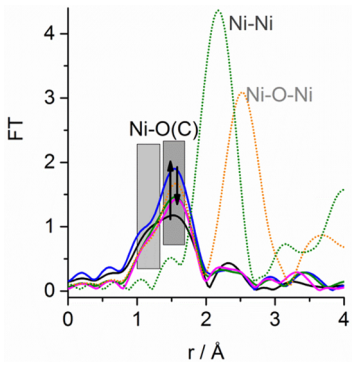

Figure 4. Fourier transform of EXAFS spectra of 0.6% Ni/SiAl in as-prepared form (black), after exposure to raffinate III at 12.4 bar and RT for 30 min (blue), after subsequent heating to 353 K (green), and after 7 h TOS at 353 K (pink). The dashed lines correspond to the references NiO (orange) and Ni foil (green). The gray fields indicate the distances found for the Ni coordination (cf. Table S2 in the Supporting Information). The arrows show the change of the amplitudes.

DOI: 10.1021/acscatal.6b02331
ACS Catal. 2016, 6, 8224−8228

Before adding butene, the coordination sphere of Ni can be fitted with two components—one with CN = 3.5 at 2.06 Å and another one with CN = 2.9 at 1.93 Å (see Figure S7 and Table S2 in the Supporting Information)—suggesting coordination to two different types of atoms, probably to O atoms of the support and to a COD or CP ligand. Note that Ni−O and Ni−C shells cannot be distinguished by EXAFS. After adding butene at RT, only the feature at 2.06 Å with a higher CN of 6.3 can be found, suggesting replacement of residual COD/Cp ligands by butene (see Figure 4, as well as Table S2). Upon heating to the reaction temperature of 353 K, a slight decrease to CN = 5.1 is observed, but without a significant change in the distance. Under reaction conditions, a dynamic change of the Ni coordination sphere is expected. These values possibly reflect the mean equilibrium geometry of the active Ni site during reaction.

When the same XAS experiment was performed in raffinate III at only 2 bar, significant differences have been observed. In the XANES spectrum (Figure S5 in the Supporting Information), an only slight rise of the white line and upshift of the absorption edge energy under raffinate III at RT indicate just minor oxidation of the initial Ni^{I} to Ni^{II}. This is initially still enhanced upon heating to 353 K; however, once this temperature is reached, a strong decrease of the white line and downshift of the absorption edge with prolonged time in raffinate III indicate a pronounced formation of Ni^{0}. This is also confirmed by the pre-edge feature, which has a tendency to approach that of the Ni foil reference with TOS at 353 K (Figure S5). Accordingly, the Fourier transform (FT) of the EXAFS spectrum shows a strong peak for a Ni−Ni shell (Figure S6 in the Supporting Information). The fact that such Ni^{0} particle formation does not occur in raffinate at 12.4 bar indicates that a high pressure is necessary to keep the Ni sites on the support isolated. Under such conditions, butene molecules are supposed to form an extended coordination sphere around the Ni single sites and prevent them from agglomerating.

To analyze the role of Ni^{II} in the catalytic reaction explicitly, a 0.6% N^{II}/SiAl catalyst was prepared with $Ni^{II}(Cp)_2$ as a precursor. This catalyst showed a similar catalytic activity as 0.6% Ni^{I}/SiAl, namely, 54% conversion after 3 h TOS, although the formation of Ni^{0} agglomerates with increasing TOS could not be completely suppressed. Interestingly, Ni^{I} species also have been detected in this catalyst after quenching (see Figure S4 in the Supporting Information). Although the spectral features do not appear exactly with the same *g*-values as in the used 0.6% Ni^{I}/SiAl catalyst (compare Figure 2c and Figure S4), the general shape of the Ni^{I} signals is comparable in both catalysts. This again suggests that a Ni^{I}/Ni^{II} redox shuttle is operating during the reaction. Interestingly, when the Ni^{II}/SiAl catalyst was prepared under aerobic conditions, no catalytic activity was observed at all, presumably because of the blockage of active Ni sites by H_2O and/or the formation of stable Ni^{II} oxide species, in which the Ni^{II} coordination sphere is saturated by O ligands and, therefore, is not prone to interact with butene molecules.

Based on *operando* EPR and *in situ* XAS measurements under elevated pressure and temperature, we can now propose a reliable reaction mechanism for butene oligomerization over supported Ni/SiAl catalysts, which involves a Ni^{I}/Ni^{II} redox shuttle (see Scheme 1). The reaction starts with the interaction of a butene π-bond with a Ni^{I} site (state (a)) and reaction with a neighboring Brønsted acid site to form a carbocation (step (a) → (b)). This view is strongly supported by the fact that no catalytic activity at all has been observed with a 0.6% Ni^{I} containing exclusively Ni^{I} single sites but no Brønsted sites (prepared via the same synproportionation method but with nonacidic SiO_2 as the support). Step (a) ⇆ (b) is reversible at low temperature and also might be the reason for the isomerization of butenes. The carbocation as an electron-poor species can react with Ni^{I} to form a Ni^{II}−R intermediate (step (c)). Upon coordination and insertion of another butene molecule (state (d)), the C8 olefin is produced by reductive elimination (state (e)) and the active site is regenerated (state (a)). The fact that only a minor percentage of the overall Ni content is detected as Ni^{I} during reaction suggests that the steady-state lifetime of states (a) and (b) is short and the sequence (b) → (c) proceeds quickly. The EPR signal of Ni^{I} most probably reflects a superposition of Ni^{I} species with a temporarily changing local environment in the early stages (states (a) and (b)) of the reaction cycle (Scheme 1). This could explain why the shape of the Ni^{I} EPR signal does not change, relative to the TOS, since it always comprises a temporal distribution of very similar species in states (a) and (b) of Scheme 1.

Scheme 1. Proposed Reaction Mechanism for Butene Oligomerization over Supported Ni/SiAl Catalysts

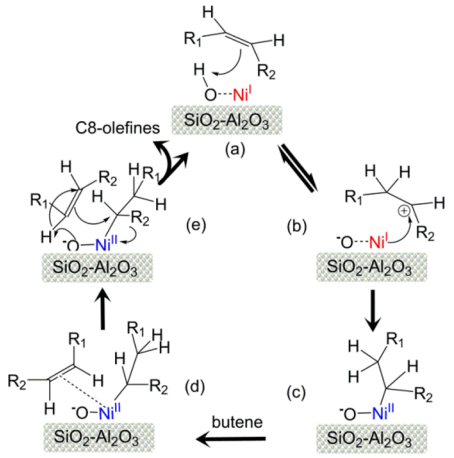

In summary, we have, for the first time, studied the dimerization of butenes from the raffinate III steam cracker fraction to C8 target products over supported Ni catalysts under industrially relevant conditions (353 K, up to 16 bar), using a novel *operando* EPR setup and *in situ* XAS spectroscopy. Active single-site Ni^{I}/Ni^{II} redox couples can only be stabilized at elevated reaction pressure but agglomerate to inactive Ni^{0} particles at $p \leq 2$ bar, clearly showing that true reaction conditions are absolutely mandatory in mechanistic studies to avoid misinterpretation.

■ ASSOCIATED CONTENT

Supporting Information

The Supporting Information is available free of charge on the ACS Publications website at DOI: 10.1021/acscatal.6b02331.

Detailed description of experimental procedures, pressure-dependent EPR spectra of adsorbed 1-butene, XAS results under 2 bar, and EXAFS fits (PDF)

DOI: 10.1021/acscatal.6b02331
ACS Catal. 2016, 6, 8224−8228

AUTHOR INFORMATION

Corresponding Authors

*jabor.rabeah@catalysis.de (J. Rabeah).
*angelika.brueckner@catalysis.de (A. Brückner).

Notes

The authors declare no competing financial interest.

ACKNOWLEDGMENTS

We thank R. Bukohl (Evonik Performance Materials GmbH), U. Marx (LIKAT) and G. Alizon (Samba Beamline, SOLEIL) for experimental help. The XAS measurements were supported by the CALIPSO Program (TNA, European Union) (Proposal No. 20130805).

REFERENCES

(1) Lappin, G. *Alpha Olefins Applications Handbook*; CRC Press: Boca Raton, FL, 1989; p 480.
(2) Brückner, A.; Bentrup, U.; Zanthoff, H.; Maschmeyer, D. *J. Catal.* **2009**, *266*, 120−128.
(3) Albrecht, S.; Kießling, D.; Wendt, G.; Maschmeyer, D.; Nierlich, F. *Chem. Ing. Tech.* **2005**, *77*, 695−709.
(4) Bonneviot, L.; Olivier, D.; Che, M. *J. Mol. Catal.* **1983**, *21*, 415−430.
(5) Ghosh, A. K.; Kevan, L. *J. Phys. Chem.* **1990**, *94*, 3117−3121.
(6) Behr, A.; Bayrak, Z.; Peitz, S.; Stochniol, G.; Maschmeyer, D. *RSC Adv.* **2015**, *5*, 41372−41376.
(7) Chauvin, Y.; Olivier, H.; Wyrvalski, C. N.; Simon, L. C.; de Souza, R. F. *J. Catal.* **1997**, *165*, 275−278.
(8) Skupinska, J. *Chem. Rev.* **1991**, *91*, 613−648.
(9) Aguayo, A. T.; Arandes, J. M.; Olazar, M.; Bilbao, J. *Ind. Eng. Chem. Res.* **1990**, *29*, 1172−1178.
(10) Garcia-Ochoa, F.; Santos, A. *AIChE J.* **1995**, *41*, 286−300.
(11) Asensi, M. A.; Martínez, A. *Appl. Catal., A* **1999**, *183*, 155−165.
(12) Nkosi, B.; Ng, F. T. T.; Rempel, G. L. *Appl. Catal., A* **1997**, *161*, 153−166.
(13) Pilbrow, J. R. *Transition Ion Electron Paramagnetic Resonance*; Clarendon Press: Oxford, U.K., 1990.
(14) Dyrek, K.; Kiessling, D.; Łabanowska, M.; Wendt, G.; Widziszewska, J. *Colloids Surf., A* **1993**, *72*, 183−190.
(15) Choo, H.; Prakash, A. M.; Park, S.-K.; Kevan, L. *J. Phys. Chem. B* **1999**, *103*, 6193−6199.
(16) Elev, I. V.; Shelimov, B. N.; Kazansky, V. B. *J. Catal.* **1984**, *89*, 470−477.
(17) Klein, A.; Kaiser, A.; Sarkar, B.; Wanner, M.; Fiedler, J. *Eur. J. Inorg. Chem.* **2007**, *2007*, 965−976.
(18) Tian, Y.; Etschmann, B.; Liu, W.; Borg, S.; Mei, Y.; Testemale, D.; O'Neill, B.; Rae, N.; Sherman, D. M.; Ngothai, Y.; Johannessen, B.; Glover, C.; Brugger, J. *Chem. Geol.* **2012**, *334*, 345−363.
(19) Shulman, G. R.; Yafet, Y.; Eisenberger, P.; Blumberg, W. E. *Proc. Natl. Acad. Sci. U. S. A.* **1976**, *73*, 1384−1388.
(20) Hoffmann, M. M.; Darab, J. G.; Palmer, B. J.; Fulton, J. L. *J. Phys. Chem. A* **1999**, *103*, 8471−8482.
(21) Sarangi, R.; Dey, M.; Ragsdale, S. W. *Biochemistry* **2009**, *48*, 3146−56.
(22) Furenlid, L. R.; Renner, M. W.; Fujita, E. *Phys. B* **1995**, *208*−*209*, 739−742.

DOI: 10.1021/acscatal.6b02331
ACS Catal. 2016, 6, 8224−8228